

Interaction of Solar Wind With Mars as Seen by Charged Particle Traps on Mars 2, 3, and 5 Satellites

K. I. GRINGAUZ

Space Research Institute, Academy of Sciences, Moscow, USSR

The near-Martian plasma measurements carried out by means of charged particle traps aboard the Mars 2, 3, and 5 satellites are reviewed. The planetary bow shock was observed; in a number of satellite passes near the planet the boundary of the obstacle that causes the bow shock was crossed. Arguments supporting the existence of an intrinsic magnetic field of Mars and of the possible existence of a quasi-isotropic plasma zone in the Martian magnetic tail are given. The behavior of the plasma and magnetic field at the obstacle boundary gives evidence favoring a magnetic nature for the obstacle (i.e., favoring the existence of a Martian magnetosphere).

1. INTRODUCTION

The USSR spacecraft Mars 2 and 3 were launched for Mars in 1971 and eventually became satellites of the planet. In 1973 the spacecraft Mars 4, 5, 6, and 7 were launched. Of these, Mars 5 became a satellite of Mars. Each spacecraft carried nearly identical charged particle traps to measure both ion and electron components of the solar wind between earth and Mars and to study plasma in the vicinity of Mars.

Because of instrument failures, only data on the electron component of the plasma were obtained by the Mars 2 and 3 spacecraft. On spacecraft launched in 1973 all particle detectors operated quite well, and electron and ion components were simultaneously measured. Results of measurements made by the above spacecraft in the vicinity of Mars have been published [Gringauz *et al.*, 1973a, b, 1974a, b, c, 1975a, b; Breus and Verigin, 1975].

The purpose of the present paper is to review the results and conclusions obtained from charged particle traps on Mars 2, 3, and 5.

2. MEASUREMENT TECHNIQUE, INSTRUMENTATION, AND DATA PROCESSING

Measurement technique, instrumentation, and some peculiarities of the data processing, including details of laboratory tests of instruments, are presented in the papers by Gringauz *et al.* [1973b, 1974a].

Each spacecraft was oriented to within $\pm 1^\circ$ of the sun-spacecraft line. One ion trap was situated on the illuminated side of the spacecraft, and one electron trap was situated on the dark side of the spacecraft (Figure 1). Angles of solar wind ion arrival are known to vary by as much as $\pm 10^\circ$ [Hundhausen, 1972]; for this reason the acceptance angle of the ion trap (a Faraday cup) was made rather large. Furthermore, the use of narrow-angle detectors for the study of solar wind ions on spacecraft accurately oriented toward the sun is not advisable without an angular scanning system (e.g., the system on the Mariner 10 spacecraft [Bridge *et al.*, 1974]). However, other experiments of Vaisberg *et al.* [1972, 1973, 1975a, b] on Mars 2-7 used electrostatic analyzers having acceptance angles of the order of a few degrees which were oriented toward the sun for the study of solar wind and Martian ion components.

Figure 2 presents a sketch of the ion trap. Figure 3 shows the angular sensitivity of the trap (the dependence of collector current on the angle between the ion velocity vector and the normal to the trap aperture at fixed ion flux and energy). The

energy analysis of ions is performed over 16 energy intervals from $e\phi_s$ to 4100 eV, where ϕ_s is the spacecraft potential. Table 1 lists the energy range for each interval. The modulation frequency is ~ 700 Hz. The measurement of one complete ion spectrum required 51 s. The interval between measurements of two successive spectra could be set to 2, 10, or 20 min. Characteristics of the trap, amplifier, and telemetry system made possible the measurement of ion fluxes ranging from $\sim 10^8$ to $\sim 10^{10}$ $\text{cm}^{-2} \text{s}^{-1}$ in each energy interval.

The electron component of the plasma was measured by a retarding potential analyzer. As was mentioned previously, this detector was on the shaded side of the spacecraft at the maximum possible distance from the spacecraft terminator and was oriented in the antisolar direction. Since solar wind electrons are essentially isotropic, this location has a negligible effect on the results of the measurements. A sketch of the electron trap is shown in Figure 4; Figure 5 shows its angular response curve. The retarding potential U_R on the Mars 2 and 3 satellites was stepped down to 70-400 V, and on Mars 4-7 to 70-300 V. A volt-ampere characteristic of the electron trap (a retardation curve) was measured during the 51-s spectral time. On Mars 2, 3, and 7 this curve was measured over 14 values of U_R , and on Mars 4-7 over 16 values. The periodicity of measurements of electron retardation curves corresponded to that of the ion energy spectra. The dynamic range of the electron collector current was from 5.5×10^{-13} to 1.55×10^{-9} A; the instrument sensitivity to an isotropic electron flux was $0.9 \times 10^6 \text{ cm}^{-2} \text{ s}^{-1} \text{ sr}^{-1}$, which takes into account the characteristics of the trap, amplifier, and telemetry system. The lower limit of currents measured by Mars 4-7 spacecraft was reduced to 3.3×10^{-13} A, which improved the isotropic flux sensitivity to $0.6 \times 10^6 \text{ cm}^{-2} \text{ s}^{-1} \text{ sr}^{-1}$.

The trap collector current is created by ambient plasma electrons, which have a Maxwellian distribution and known bulk velocity relative to the spacecraft frame. Using trap characteristics obtained from laboratory calibration, Gringauz *et al.* [1974b] give formulas for the dependence of the collector current on U_R .

From an analysis of the volt-ampere characteristic curve one may use the retarding potential method to determine the particle density (in our case the electron density n_e) and temperature T_e . Gringauz *et al.* [1974b] have shown that if the bulk velocity V is taken to be 450 km s^{-1} , the error in determining T_e owing to a poor choice of V in the range $300 < V < 600 \text{ km s}^{-1}$ does not exceed 5%. (It should be kept in mind that in processing electron data from Mars 2 and 3 the authors did not have any data on the value of V from ion energy spectra

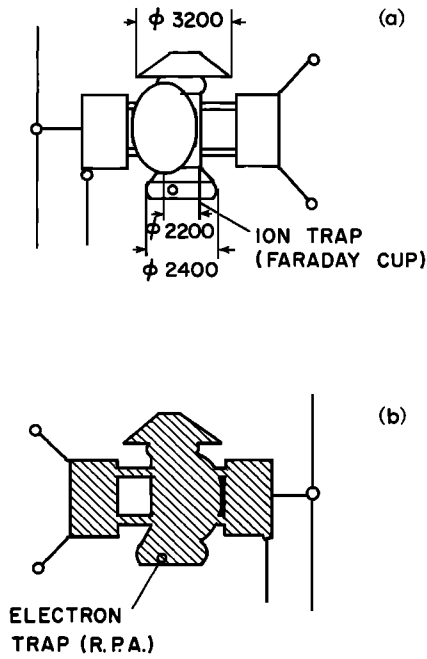


Fig. 1. (a) Location of the ion traps (Faraday cups) on the illuminated parts of spacecraft launched to Mars in 1971-1973. (b) Location of electron traps (retarding potential analyzers) on the shadowed parts of the same spacecraft. The traps are oriented in the antisolar direction and are located far from the terminators of spacecraft.

measurements.) Figure 6 presents some samples of electron retardation curves obtained along the earth-Mars path by the Mars 4-7 spacecraft [Gringauz *et al.*, 1974a]. Solid curves are calculated from formulas derived by Gringauz *et al.* [1974b]. Most of the experimental points lie on the calculated curves. However, near zero retarding potential the experimental current values considerably exceed their calculated values (Figure 6, shaded regions). According to Whipple and Parker [1969], this behavior is due to the detection of photoelectrons and secondary electrons from spacecraft surfaces. Comparison of the curves in Figure 6 with similar retardation curves of the electron trap on the Ogo 1 satellite [Whipple and Parker, 1969] demonstrates that the trap on board the Mars spacecraft was less influenced by photoelectrons and secondary electrons than was that aboard the Ogo 1.

Gringauz *et al.* [1974b] have shown that by choosing rather high values of the retarding potential U_R it is possible to neglect the influence of spacecraft potential ϕ_s in determining T_e . Then the maximum current in the electron trap at zero retarding potential is $I_{max} \approx An_e T_e^{1/2}$, where $A = const$ [Gringauz *et al.*, 1974b]. Thus I_{max} depends mainly on n_e . As can be

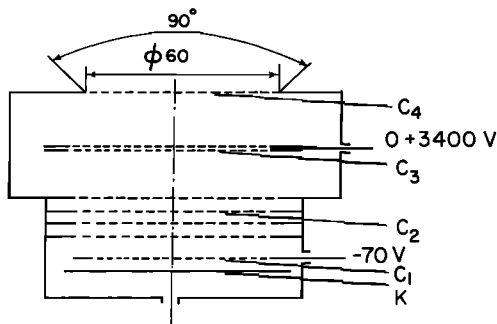


Fig. 2. Sketch of the Faraday cup. C₃ is the modulation grid, C₁ the suppressor grid, and K the collector.

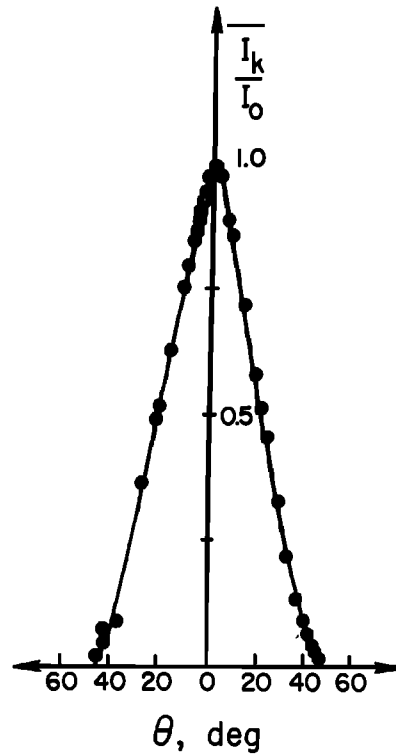


Fig. 3. Acceptance angle diagram of the Faraday cup shown in Figure 2, taken from laboratory test data.

seen from Figure 6, photoelectrons from the sunlit side of the spacecraft and secondary electrons make some contribution to I_{max} . This contribution is fairly constant, since the orientation of the spacecraft relative to the sun was unchanged during the measurements and since the intensity of solar radiation causing photoemission is very stable [Heath, 1973]. As will be shown below, variations in I_{max} near the planet are large (about 1 order of magnitude). These variations cannot be explained by photoemission variations but rather must correspond to changes of electron fluxes in the ambient plasma.

The determination of n_e from a retardation curve is more sensitive to ϕ_s than to T_e . Admitting some uncertainty in ϕ_s , one can estimate n_e from trap retardation curves with an uncertainty of about a factor of 2 [Gringauz *et al.*, 1974b].

The method for deriving ion energy spectrum measurements by means of ion trap modulation has been used successfully on many spacecraft and in our opinion needs no additional explanation.

3. RESULTS OF MEASUREMENTS

Table 2 gives the dates on which the three spacecraft being considered were placed into Mars orbit. Initial orbital param-

TABLE 1. Energy Intervals for Ion Detector

Interval	Width of Interval, V	Interval	Width of Interval, V
1	0-40	9	932-1195
2	40-70	10	1190-1500
3	70-103	11	1500-1835
4	103-200	12	1845-2225
5	200-332	13	2225-2625
6	332-500	14	2600-3060
7	500-700	15	3010-3550
8	700-932	16	3550-4100

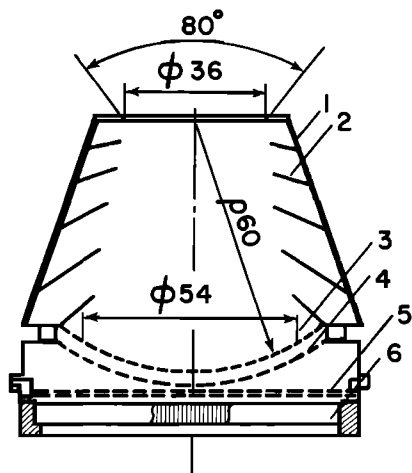


Fig. 4. Sketch of the electron retarding potential analyzer: 3 and 4 are the analyzing grid systems (spherical), 5, the suppressor grid, and 6, the collector.

ters are also given. The electron trap data from the Mars 2 and 3 satellites were obtained during the period November 1971 to January 1972. The ion and electron data from the Mars 5 satellite were obtained during the period February 13–26, 1974. The following analysis will employ the coordinates $(x, (y^2 + z^2)^{1/2})$, where the x axis passes through the planet center and points toward the sun and $(y^2 + z^2)^{1/2}$ is a radial distance perpendicular to the x axis. In this coordinate system the motion of Mars around the sun displaces the orbits of each spacecraft relative to a stationary frame. Figure 7 shows one orbit of Mars 2 and its precession in the above coordinate system. For comparison, near-Mars portions of a Mars 2 and a Mars 5 orbit are presented in Figure 8 in the same coordinates. Let us call that part of near-Mars space to the right of the terminator plane the antisolar part. Figures 7 and 8 show that the Mars 5 satellite penetrated the antisolar region to within 6000 km of the x axis and to within distances of the order of 10^4 km from the terminator ($x = 0$) plane; during this penetration, data from electron traps were obtained from Mars 2 and 3.

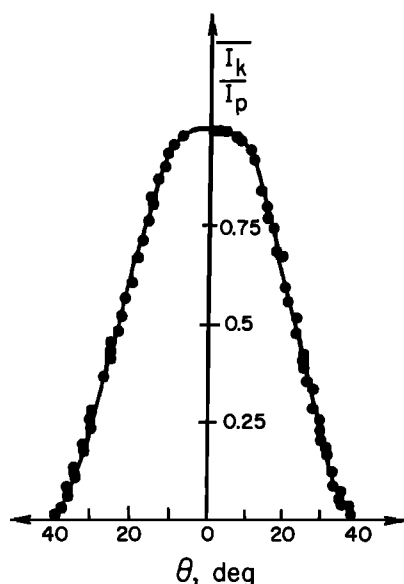


Fig. 5. Acceptance angle diagram of the electron trap shown in Figure 4, taken from laboratory test data.

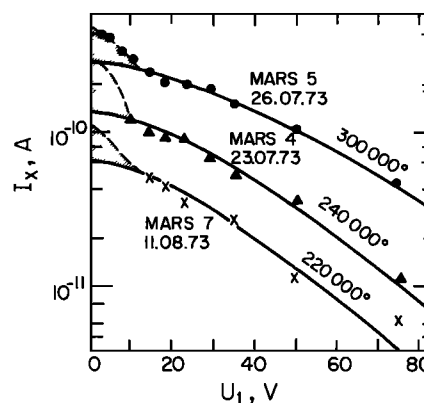


Fig. 6. Samples of electron retardation curves obtained during flights of Martian spacecraft while they were close to the earth's orbit. Above each curve the corresponding electron temperature value is given. The increased slope of the part of each curve corresponding to retarding potentials below 10 V is due to photoelectrons emitted from sunlit parts of the spacecraft.

Plasma Electron Component Measurements

During the four orbits of Mars 3 shown in Figure 7, repeated variations of the electron density n_e and the electron energy distribution were measured. In the preliminary analysis of results [Gringauz et al., 1973a] the Mars 3 orbits were conditionally divided into four characteristic zones, marked by the letters A–D on the second orbit of Mars 3 in Figure 7. Samples of retardation curves typical of each zone are shown in Figure 9. Zone A corresponds to the inbound portion of the orbit. The lowest values of I_{max} (the collector current at zero retarding potential) and the lowest values of E_R (the retarding potential at which the current became lower than the instrument sensitivity threshold) are typical of this zone. Typical values of n_e and T_e on the inbound parts of the orbits were $n_e \sim 3\text{--}6 \text{ cm}^{-3}$ and $T_e \sim 60\text{--}100 \times 10^8 \text{ }^\circ\text{K}$. The distribution function was Maxwellian (that is, the shape of the retardation curve corresponded to that calculated under the assumption of a Maxwellian distribution). Suprathermal 'tails' are absent in the range of instrument sensitivity. The retardation curves had the same form when Mars 2 and 3 approached the planet prior to establishing orbits around Mars. During data processing the plasma in zone A was identified with the undisturbed solar wind [Gringauz et al., 1973a].

When Mars 3 entered zone B near the pericenter of its orbit (Figure 7), the form of the retardation curves changed suddenly. I_{max} and E_R increased, and intense suprathermal tails appeared, as did electrons with energies of $>50 \text{ eV}$. (Such electrons were absent in the undisturbed solar wind observed in Mars orbit.) The transition from zone A to zone B was determined to be a bow shock arising from the flow of the solar wind around the planet, and zone B was interpreted as a transitional region [Gringauz et al., 1973a, b, 1974a].

Enhanced values of n_e and T_e and the simultaneous appear-

TABLE 2. Appropriate Orbital Data for Mars Spacecraft

Date of Orbit	Periapsis,		Period of Revolution			
	km	Apsis, km	d	h	m	
Mars 2	Nov. 27, 1971	4800	28,000	17	55	
Mars 3	Dec. 12, 1971	4650	212,000	12	16	30
Mars 5	Feb. 13, 1974	1800	32,000	25		

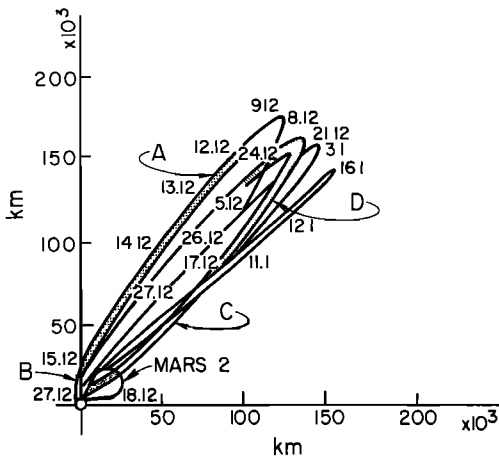


Fig. 7. The orbits of Mars 2 and 3 satellites in December 1971 and January 1972.

ance of suprathermal electrons (energies of $>50-100$ eV) in zone B and near the apocenter (the outbound parts of Mars 3 orbit) initially caused some suspicion that the enhancements might have been related to spatial instead of temporal variations of the plasma [Gringauz et al., 1973a]. Further analysis [Gringauz et al., 1973b, 1974a] showed that this impression was misleading, since very intense interplanetary shock waves reached Mars during the outbound portion of the Mars 3 orbit and near the apocenter. The velocities of these disturbances were determined from data of satellites orbiting Mars and earth. It is interesting to note that owing to angular 'lag' of Mars relative to earth during the period of measurement (early 1972), corotation of solar plasma streams caused these disturbances to be observed near Mars several days before they were observed at earth [Gringauz et al., 1973b, 1974a].

On the majority of passes of Mars 2 and 3 near the planet all plasma and magnetic field detectors were switched off near orbital pericenter; therefore only one crossing of the bow shock was registered by these spacecraft during their entry into the transitional region between zones A and B. The transitional region and the 'obstacle' creating the bow shock were not detected by these spacecraft except in a few cases described below. The plasma and magnetic instruments aboard Mars 5 were not switched off near the pericenter.

One of the instances in which the plasma detectors aboard Mars 2 were switched on near orbital pericenter took place on

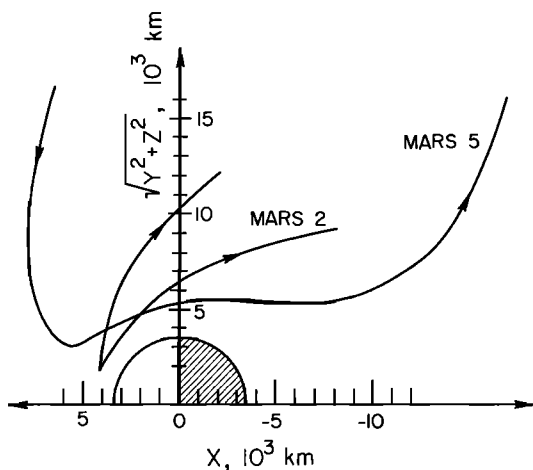


Fig. 8. Near-planetary parts of orbits of Mars 2 (1972) and 5 (1974) satellites.

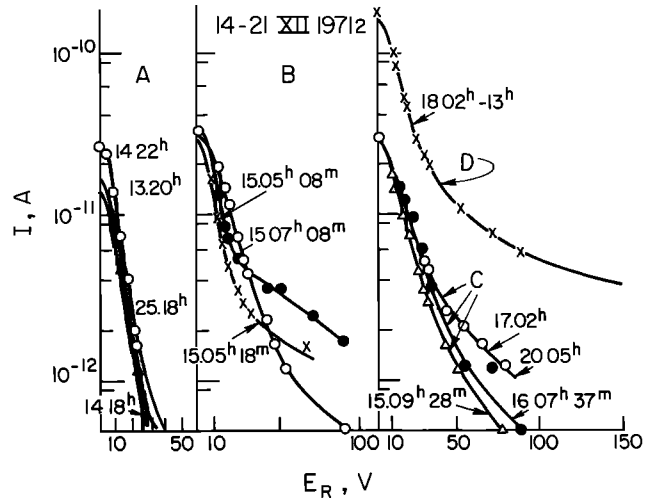


Fig. 9. Electron retardation curves obtained from Mars 3 satellite at different parts of orbit, designated in Figure 7 as A, B, C, and D.

January 8, 1971. Results of simultaneous electron and magnetic field measurements during this orbit were considered in detail by Breus and Verigin [1975]. Variations of collector currents of the trap at the retarding potentials $E_R = 8, 20,$ and 50 V are shown in Figure 10. These data were taken while Mars 2 was near its pericenter (Figure 11). The upper part of Figure 10 shows the simultaneous variations of the magnetic field [Dolginov et al., 1973, 1975]. Interval 1 in Figures 10 and 11 corresponds to the crossing of the bow shock according to the response of the electron detector. This interval coincided with the interval in which the magnetic field magnitude $|\vec{B}|$ increased substantially. During interval 2 an abrupt and substantial decrease of electron fluxes occurred; fluxes of electrons with energies of >50 eV were especially decreased. Apparently, this interval corresponds to the boundary of the obstacle which creates the Martian bow shock. Decreased electron fluxes were measured until interval 2', at which point the fluxes increased substantially. Between intervals 2 and 2' the highest values of $|\vec{B}|$ seen during the orbit were measured ($|\vec{B}| \sim 20-25 \gamma$). Following 2' the current from electrons with energies of >50 eV fell to $\sim 10^{-12}$ A; the value of $|\vec{B}|$ fell an order of magnitude in comparison to its value in the region between 2 and 2' and eventually reached the magnitude of the interplanetary magnetic field ($\sim 2 \gamma$). Magnetic field investigators believe that interval 1 corresponds to the crossing of the near-planet bow shock, that the region between intervals 1 and 2 corresponds to a Martian magnetosheath, and that the region between intervals 2 and 2' corresponds to the Martian magnetosphere. It is evident that the behavior of the plasma electron component during that portion of the Mars 2 orbit under consideration does not contradict such an interpretation.

Another case in which plasma and magnetic devices were not switched off near the planet took place on January 21, 1972, on the Mars 3 satellite. As was shown by Gringauz et al. [1974a], the growth of electron fluxes and the appearance of energetic electrons corresponded to the satellite's crossing the bow shock as determined by magnetic field data; the decrease of electron fluxes corresponded to the satellite's being inside the 'magnetosphere.'

Since in the majority of passes of Mars 2 and 3 the plasma devices were switched off inside the transitional region so that measurements inside the obstacle were not performed, the origin of the obstacle can be determined only from the posi-

tions of the bow shock crossings. Various hypotheses about the nature of the obstacle lead to different bow shock crossing distances. Hypotheses which predict crossing distances that contradict observed crossing distances may be rejected. This problem will be discussed below.

As was mentioned, the plasma and magnetic devices on Mars 5 were not switched off near the planet, and in a number of cases the spacecraft successively detected the bow shock, the inner boundary of the transitional region (i.e., the outer boundary of the obstacle), a second entry into the transitional region, and finally the undisturbed solar wind. Because of peculiarities of the Mars 5 orbit (Figures 12 and 16) the satellite always entered the region of the obstacle in the antisolar part of near-Mars space. Characteristics of electron as well as ion fluxes were obtained by means of wide-angle charged particle traps. Figure 12a shows the orbit of Mars 5 on February 14, 1972, in solar ecliptic coordinates (x, y, z) (the x axis is directed toward the sun, the y axis lies in the Mars orbital plane and makes a blunt angle with the velocity vector of the planet, and the z axis completes the right-hand system of rectangular coordinates). In Figure 12b the near-planet part of the same orbit is presented in $(x, (y^2 + z^2)^{1/2})$ coordinates.

The analysis of the electron trap obtained 2 years later by Mars 2 and 3 in the undisturbed solar wind showed electrons which in the majority of cases had a Maxwellian distribution (in the range of instrument sensitivity) without suprathermal tails. Measurements were taken with the potential of complete retardation (>40 V). The crossing of the bow shock was always followed by the abrupt growth of electron fluxes (i.e., by growth of I_{\max}), a rise in electron temperature T_e , and the appearance of suprathermal tails due to electrons with energies greater than 50–100 eV. On Mars 5, crossings of the inner boundary of the transitional region, i.e., satellite entries into the obstacle region (the magnetosphere), were also systematically registered by the electron component data. This transition can be recognized by the decrease of electron fluxes (as

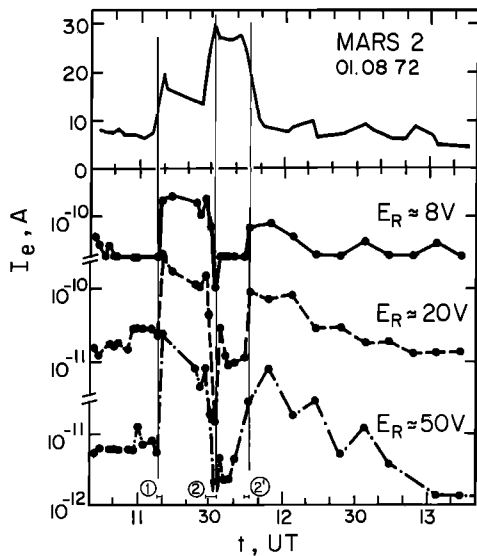


Fig. 10. Variation of magnetic field value B and electron currents (created by electrons with energies greater than 8, 20, and 50 eV, respectively) at the planetary part of Mars 2 orbit on January 8, 1972. At the bow shock crossing (point 1) the values of B and electron currents increased simultaneously; near point 2, B increased, and the electron current decreased, as occurs after the earth's magnetopause crossings. Near point 2', B decreased, and electron currents increased as the satellite went out of the Martian magnetosphere.

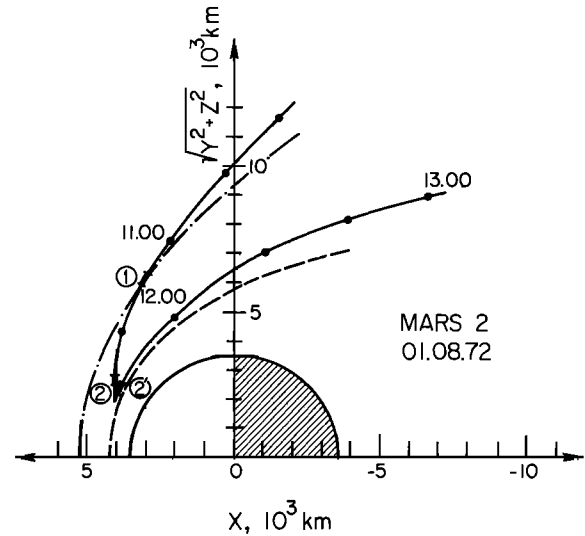


Fig. 11. The near-planetary part of the Mars 2 satellite orbit on January 8, 1972, showing spacecraft crossings of the bow shock and the obstacle boundary (corresponding to Figure 10 data).

reflected in I_{\max}) in comparison to those in the magnetosheath and by the decrease of electron energies. However, both fluxes and energies in this region remained higher than those in the undisturbed solar wind. When the satellite had passed several thousand kilometers inside the obstacle, the spacecraft again entered a transitional region.

The lower part of Figure 13 presents typical samples of retardation curves obtained from Mars 5 in the undisturbed solar wind, the magnetosheath, and inside the obstacle on the antisolar side of space near Mars. The upper part of the figure gives the ion spectra obtained simultaneously from the Faraday cup.

Measurements of Ion Component, Comparison With Magnetic Measurements

As a rule, the ion spectra registered by the modulation method employing a Faraday cup in the solar wind exhibit a peak created by α particles as well as a proton peak, and this allows one to determine the ion flux, ion bulk velocity, density, temperature, α particle density, and solar wind ram pressure. The ram pressure is a particularly important parameter for the study of the near-planet bow shock.

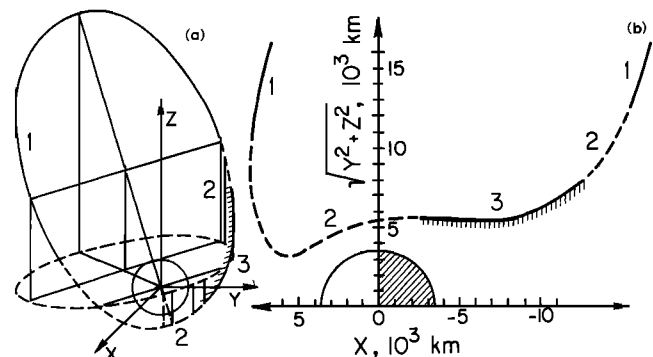


Fig. 12. One of the Mars 5 satellite orbits, (a) in the solar ecliptic coordinate system and (b) in the $x, (y^2 + z^2)^{1/2}$ system. Zone 1 corresponds to the undisturbed solar wind, zone 2 to the transition region (magnetosheath), and zone 3 to the obstacle (magnetosphere). Note that zone 3 corresponds to low aerographic latitudes.

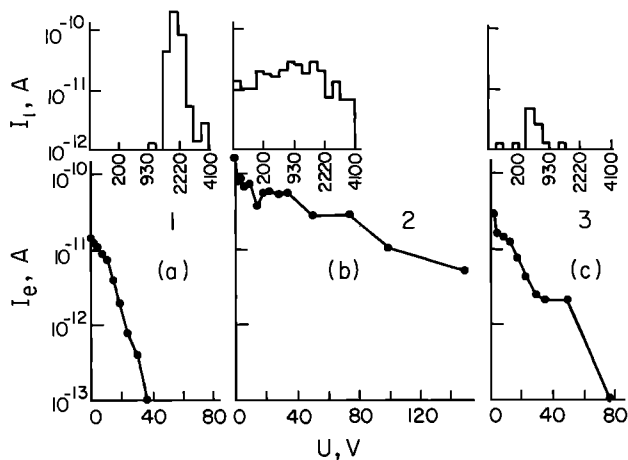


Fig. 13. Samples of ion spectra (top part of figure) and electron retardation curves from the Mars 5 satellite corresponding to zones (a) 1, (b) 2, and (c) 3, indicated in Figure 12.

When the spacecraft crossed the shock, the form of the ion spectra widened owing to the thermalization of ions (upper part of Figure 13b). The change of the form of the ion spectrum occurred simultaneously with the change of the form of the electron retardation curve. (It should be kept in mind that one complete measurement of the ion spectrum required 51 s.)

When the spacecraft crossed the inner boundary of the transitional region on the antisolar side of near-Mars space (i.e., during entry into the antisolar part of the obstacle), ion currents decreased so significantly that in approximately 30% of the cases the ion fluxes were below instrument sensitivity, and in only 40% of the cases were the ion fluxes reliably registered (the sensitivity of the detector was 3 or more times greater than the minimum telemetric reading).

In Figure 14, ion spectra are shown which were registered during a number of passes of Mars 5 near the planet from February 13–26, 1974 [Gringauz *et al.*, 1975b]. Rows of spectra are shifted so that the passes of the satellite through the inner boundary of the transition region (into the obstacle) are matched to the vertical line indicating the magnetopause (mp).

On February 13, 14, 15, 21, and 24, measurements were begun in the undisturbed solar wind; on February 20, 25, and 26, detectors were switched on when the satellite was already

at the obstacle boundary or inside it. On February 19, measurements were performed during a large interplanetary disturbance when fluxes and energies of solar wind ions were anomalously high. Evidently owing to this disturbance the ion fluxes inside the obstacle were higher than those in all other cases. However, it may be that the obstacle was so compressed that the satellite passed outside it.

From ion spectra of Figure 14, obtained on February 13 and 14, one can distinctly see that the satellite successively crossed the bow shock, crossed the obstacle boundary, went out of the obstacle, entered the transitional region and recrossed the bow shock, and finally reentered the undisturbed solar wind. The orbits of Mars 5 for February 13 are given in Figure 16a.

Empty squares after the mp line in Figure 14 correspond to ion fluxes inside the obstacle which were below instrument sensitivity threshold. When ions are detected inside the obstacle, their energies are, as a rule, lower than the solar wind. For example, spectra 18 for February 14, 1974, and 13 for February 20, 1974, in Figure 14 demonstrate this behavior.

It is important to note that during all passes of the satellite inside the antisolar part of the obstacle, electron fluxes and energies were always substantially lower than those in the transitional region (magnetosheath) but somewhat higher than those in the undisturbed solar wind (see the typical retardation curve in Figure 13b).

Comparison of results of simultaneous magnetic field measurements conducted from the Mars 5 satellite by Dolginov *et al.* [1973] showed the following results.

1. The boundaries of parts of orbits with different plasma characteristics coincided with boundaries having different magnetic field characteristics.

2. During the measurement of undisturbed solar wind particles by means of wide-angle traps, the magnetometer found a magnetic field with small fluctuations, typical of interplanetary space.

3. After a satellite crossed the bow shock the magnetic field and its fluctuations substantially increased; the x component of the interplanetary field did not change sign.

4. Inside the obstacle (to the right of the mp line in Figure 14) the magnetic field continued to increase, its fluctuations became smaller, and its x component always maintained the same direction of the interplanetary magnetic field. After the spacecraft left the obstacle the magnetic field decreased, its

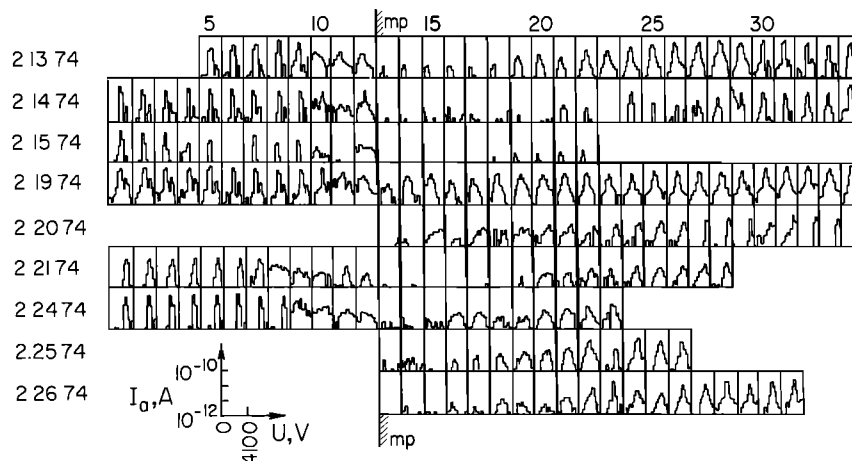


Fig. 14. Ion spectra from the Mars 5 satellite obtained during measurements near the planet; mp designates the magnetopause. Rows of spectra are shifted so that crossings by the satellite of the inner boundary of the transition region (magnetopause) are matched.

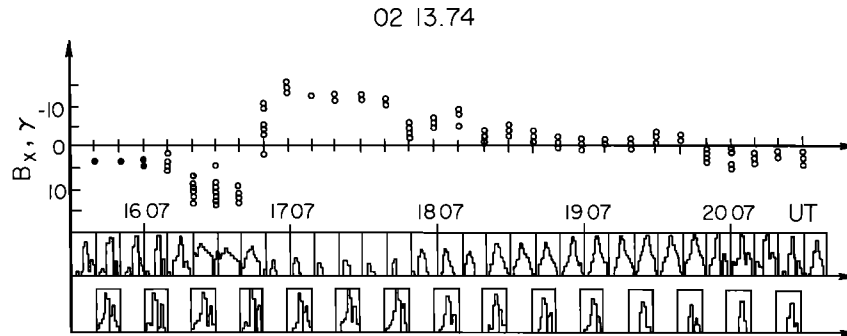


Fig. 15. Simultaneous data from February 13, 1974, showing discretely continuous component of the magnetic field from the Mars 5 satellite (top part of figure), an ion spectrum from the Mars 5 satellite, and an ion spectrum from Mars 7 spacecraft, which was at the time at a distance of 5×10^6 km from the planet (bottom part of figure).

fluctuations increased, and the x component direction corresponded to the direction of the appropriate component of the interplanetary field.

To illustrate the above behavior, the results of simultaneous measurements of the ion plasma component (the number of continuous spectra) and magnetic field component B_x are presented in Figure 15; the data were obtained on February 13, 1974 [Gringauz *et al.*, 1975b]. One can see the characteristic changes of ion spectra, the growth of the x component of the magnetic field, and the increase of its fluctuations observed during the satellite entry into the transition region at 1627 UT. At 1657 UT, when an abrupt increase of ion fluxes was observed, B_x changed sign and up to 1757 UT kept the same sign and fluctuated less than it did in the transitional region. At 1757 UT, ion fluxes again simultaneously increased with the increase of magnetic field fluctuations (the satellite entered the transitional region).

For comparison, the lower part of Figure 15 shows ion spectra which were obtained from the Mars 7 spacecraft, which on February 13, 1974, was at a distance of 5×10^6 km from the planet. These spectra, as well as spectra obtained before or later than the time interval of Figure 15, do not reveal any peculiarities in the solar wind analogous to those observed in the near-planet plasma.

4. DISCUSSION OF RESULTS

The previous sections described the results of measurements carried out by the wide-angle charged particle detectors on board Mars 2, 3, and 5. All of these spacecraft detected the electron component, while only Mars 5 detected ions as well as electrons. Particle fluxes and energies were measured over the orbits of these satellites. The coordinates of some bow shock crossings and of the surface of the obstacle creating this bow shock were obtained, and some measurements were performed inside this obstacle.

There can be no doubt of the existence of a bow shock near Mars, since it was detected by the simultaneous measurements of three groups of experimenters led by Gringauz, Vaisberg, and Dolginov. The main problem remaining is the nature of the obstacle producing this bow shock.

It is appropriate to compare the results of measurements made near Mars with similar ones made near the earth and to review the different models suggested to describe the flow of the solar wind around Mars.

First, let us review some data on the near-earth bow shock and the terrestrial magnetosphere.

According to plasma and magnetic measurements from the Imp satellites [Olbert, 1968; Fairfield, 1971] and the plasma

measurements from the Prognoz and Prognoz 2 satellites [Bezrukikh *et al.*, 1975], the geocentric distance to the subsolar point of the near-earth bow shock averages $\sim 14 R_E$. This distance may vary from 11 to $21 R_E$, and so the variation in bow shock distance is $\Delta R_{BS,E} \sim 10 R_E$. The mean geocentric distance to the magnetopause subsolar point R_{0E} is $\sim 10 R_E$, and so $\Delta R_{BS,E} \sim R_{0E}$. Variations in the solar wind ram pressure ρv^2 are the main reason for the bow shock motions; the change of the interplanetary magnetic field direction is an additional reason. Since velocity v is practically constant but ρ changes by about a factor of 2 between earth and Mars, the solar wind ram pressure at Mars is about one half the ram pressure at earth. Thus the relative variations of ρv^2 near Mars are the same as those near earth, while the absolute variations are half those near earth. If one assumes that the physical nature of the obstacle near Mars is the same as that near earth (i.e., an intrinsic dipole magnetic field), it is reasonable to expect that the range of aerocentric distances to the Martian bow shock subsolar point caused by variations in ρv^2 will also be such that $\Delta R_{BS} \sim R_0$, where R_0 is the mean aerocentric distance to the subsolar point of the Martian magnetopause. The data indicate that R_0 is only ~ 500 – 1000 km greater than the Martian radius R . (This is easily seen from Figure 16a, in which the Mars 5 orbit of February 13, 1974, is shown. The hatched orbit section is located inside the obstacle; the boundaries of this section are points on the obstacle surface. It is evident that even inside the antisolar (tail) portion the radius of the obstacle is only a few hundred kilometers greater than R .) It should be expected that ram pressure variations can shift the bow shock by distances of the order of R ; i.e., $\Delta R_{BS} \sim 4000$ km.

Before returning to the results of the measurements by the wide-angle plasma detectors on board the Mars satellites, one should note that the plasma and magnetic field investigators (headed by Gringauz, Dolginov, and Vaisberg) have compared all the primary data available from the three satellites and have found complete agreement between the plasma and magnetic field boundaries (i.e., the positions of the bow shock and the obstacle boundaries). Comparison of the results of measurements from wide-angle detectors [e.g., Gringauz *et al.*, 1975a, b] to the data obtained by means of narrow-angle electrostatic analyzers [e.g., Vaisberg, 1973, 1974] has been discussed in the literature.

The three groups of experimenters mentioned above have made attempts to define the values of ΔR_{BS} and R_0 , using the coordinates of points at which the satellites crossed the Martian bow shock. Unfortunately, these authors used in their various papers different expressions relating the parameters of

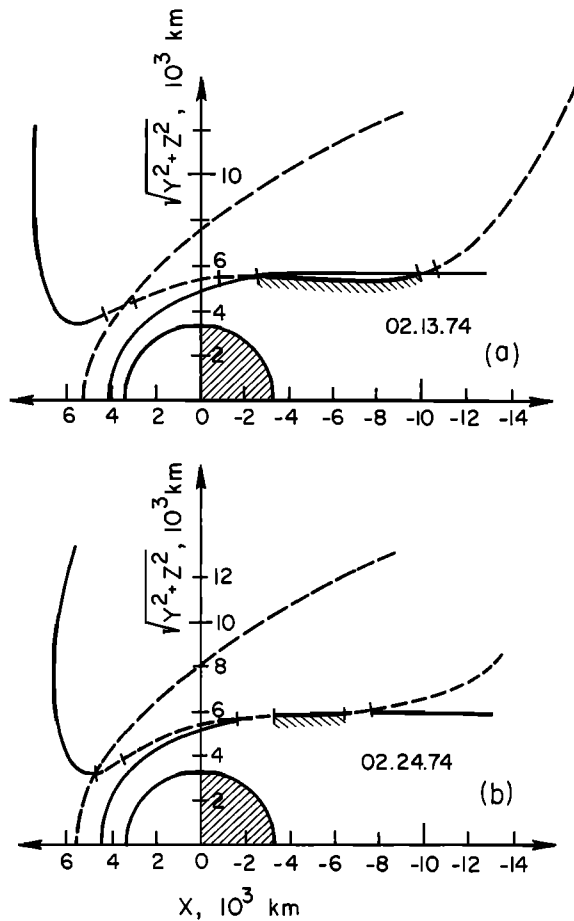


Fig. 16. Near-planetary parts of Mars 5 satellite orbits on February 13 and 24, 1974. The hatched sections of the trajectory correspond to space inside the obstacle (magnetosphere).

the plasma flow, the size and shape of the obstacle, and the coordinates of points at the bow shock. Among the expressions used were formulas from *Obayashi* [1964] and *Holzer et al.* [1972] and the results of calculations by *Spreiter et al.* [1970]. In these articles, various shapes of the obstacle were assumed. The Martian bow shock was analyzed by assuming a spherically shaped obstacle similar to that characterizing the earth; also an analysis was conducted assuming an elongated obstacle which was less expanded than that in the case of the earth. The characteristics of the plasma flow around the planet and its influence on the bow shock position were also in most cases unknown and were chosen more or less arbitrarily. For example, *Gringauz et al.* [1973b, 1974b] used a Mach number of $M_\infty = 8$, while *Vaisberg and Bogdanov* [1975] used $M_\infty = 5$. The solar wind ion density could be determined only from Mars 5 by means of the Faraday cup, and the angle of arrival of the solar wind fluxes could not be determined by any experiment under consideration.

The shape of the obstacle is not well known. The twofold entries into the antisolar part of the obstacle (the tail) by Mars 5 (Figure 16) show that the tail expands with distance along the x axis much less than would be the case for the tail of the earth's magnetosphere. If the arguments of *Rassbach et al.* [1974] are correct, one can expect that the shape of the subsolar part of the obstacle can vary, depending on the relationship between the pressure of the intrinsic planetary magnetic field and the solar wind ram pressure. Therefore one should not place too much confidence in the values of the bow shock

distances or in the characteristics of the obstacles as determined by the data taken by the Martian satellites. That different distances are given by different authors is rather immaterial. A much more essential point, in our opinion, is that all three groups of investigators concur that R_{BS} and R_0 vary over a wide range.

Figure 17 [*Gringauz et al.*, 1975b] shows a number of near-planetary sections of the Mars 2, 3, and 5 orbits within which bow shocks were crossed. The length of each section is determined by the time between consecutive measurements of charged particle energy spectra of a given pass. Clearly, no calculations are required to show that the bow shock location varied considerably.

According to the estimate made by *Gringauz et al.* [1975b] from data of the first Mars 5 bow shock crossing, R_{BS} varies from 2.2 to 1.5 R . The attempts to plot a bow shock based on two points where Mars 5 crossed on some of its passes implied an obstacle with its subsolar point placed under the surface of the planet. This implication demonstrates the uncertainty of the information on the shape of the obstacle, an uncertainty already mentioned above.

According to estimates made by *Vaisberg and Bogdanov* [1975], R_{BS} values determined from Mars 2 and 3 data varied from 2 R to R .

Thus the experimental data confirm that if the obstacle creating the bow shock is the dipole magnetic field of Mars, then the range over which aerocentric distances of the subsolar point of a shock wave may vary (ΔR_{BS}) should be of the order of 1 R .

Note that as shown by *Gringauz et al.* [1975b], the values of R_{BS} and R_0 found from the Mars 5 data should increase with decreasing solar wind ram pressure. On February 19, 1974, it was found that $R_0 = 4175 \pm 75$ km and $\rho v^2 = 4.2$ dyn cm^{-2} , and two days later on February 21, that $R_0 = 4475 \pm 75$ km when $\rho v^2 = 1.2$ dyn cm^{-2} . The ram pressures were determined from data obtained with the Faraday cup.

Unlike the widely changing positions of bow shocks and the size of the obstacle creating the bow shock the day side iono-

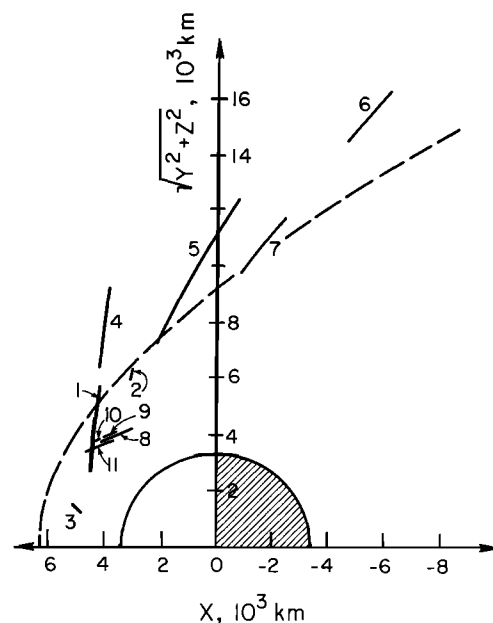


Fig. 17. Segments of satellite orbits for which crossings of a Martian bow shock were observed.

sphere of Mars is stable, as was confirmed by long-term observations of Mariners 7 and 9 radio occultations [Kliore *et al.*, 1972, 1973]. In the period 1969–1971 the ionosphere had a maximum electron concentration of $n_e \sim 10^8 \text{ cm}^{-3}$ at a height of about 150 km and a scale height of 40 km. This measurement implies that n_e amounts to only several particles per cubic centimeter (if not less) and cannot balance the pressure of the solar wind. Even if Mars has no ionosphere similar to the earth's plasmapause and even when a height variation of n_e is considered, the Martian ionosphere still cannot generate sufficient pressure to stand off the solar wind. Hence the model of the interaction of the solar wind with the Martian ionosphere by Spreiter *et al.* [1970] and Spreiter and Rizzi [1972], in which the ionosphere acts as an obstacle creating a bow shock and the ionospheric plasma pressure balances that of the solar wind, is not valid for Mars (although the model may be valid for Venus [Ness *et al.*, 1974]).

Other versions of an ionospheric obstacle in the absence of a magnetic field of Mars are those in which the obstacle is fully or partially created by a magnetic field induced in the ionosphere by the solar wind flow around it [e.g., Michel, 1971; Cloutier and Daniell, 1973]. In most cases the models have not been developed so that they could be used with known solar wind parameters (velocity and pressure) to calculate the subsolar heights of the obstacle and of the bow shock (R_0 and R_{BS}) on the basis of characteristics of the Martian ionosphere.

Only Cloutier and Daniell [1973] give estimates of the heights of the obstacle ('ionopause') for Mars when the presence of an ionospheric system is taken into account. Calculated heights (350–425 km) are insufficient to create a bow shock of the kind sometimes observed from Martian satellites. The observed bow shocks had subsolar points of the order of several thousands of kilometers from the planet.

The stability of the Martian ionosphere provides evidence against the possibility of substantial solar wind effect on the structure of the Martian ionosphere (as has been supposed by Cloutier *et al.* [1969]).

At present, there is no known experimental fact which contradicts the concept of an intrinsic Martian magnetic field. Plasma and magnetic measurements with high time resolution at low altitudes are needed for detailed study of the peculiarities of physical processes near Mars. However, the totality of results obtained from Soviet Martian satellites leaves little doubt about the existence of an intrinsic Martian magnetic field.

The existence of a dipole magnetic field implies, as in the case of the earth, a process of reconnection of interplanetary and planetary magnetic field lines as well as plasma convection inside the Martian magnetosphere. Owing to the small value of the intrinsic magnetic dipole moment, external forces should cause many more distortions of the Martian magnetosphere than occur at the same distances for earth. Variations of the solar wind pressure and the interplanetary field should cause substantial variations of the size and, possibly, the shape of the Martian magnetosphere; these variations are apparently displayed as variations of the bow shock subsolar distance, which can change by some thousands of kilometers. It is possible that very high solar wind ram pressures cause the Martian magnetopause to move down to ionospheric altitudes. Estimates of the convection velocity in the Martian magnetosphere and of the magnetospheric shape made by Rassbach *et al.* [1974] seem reasonable.

Let us consider the physical characteristics of plasma in the antisolar part (tail) of the Martian magnetosphere, using data

obtained from the Mars 5 satellite [Gringauz *et al.*, 1974c, 1975a, b]. When a large sharp decrease of ion currents in the Faraday cup occurs (large in comparison to fluctuations in the undisturbed solar wind), the electron trap currents remain essentially unchanged. (They may even be slightly larger in comparison to currents of the solar wind, as can be seen in Figure 13.) Thus the plasma concentration must also be almost unchanged. This can take place in two ways: either the ion flux changes its direction (a rather considerable change must occur, since the ion trap acceptance angle is wide), or the ion flux becomes quasi-isotropic. Let us note that a change in the direction of the plasma motion or isotropization of ion flux should appreciably influence only the ion currents registered; electron currents would not be affected, since the electron flux is almost always isotropic, even in the undisturbed solar wind. Ion flux isotropization should decrease the trap ion current by 20 times in comparison to cold ion flux normal to the trap aperture (instrument performances were discussed in section 2 of this paper). The probability that the mean ion energy E increases to values beyond the energy range of the instrument ($E \leq 4.1 \text{ keV}$) is low, since nearly all registered variations of ion spectra in the Martian magnetospheric tail are within the energy interval 200–500 eV. Let us note, however, that in the moments when there are no readings registered the possibility of such an increase in energy E cannot be excluded.

We cannot comment on the nature of the plasma in the antisolar region under consideration [see Gringauz *et al.*, 1975b]. One can consider this region as either a plasma sheet similar to the one existing in the central part of the earth's magnetotail [Gringauz, 1969] or as a boundary layer adjacent to the Martian magnetopause. This layer would be similar to that found in the tail of the earth's magnetosphere [Hones *et al.*, 1972; Akasofu *et al.*, 1973].

If the boundary layer interpretation is correct, then the plasma flow direction in this region should be mainly antisolar, although near the earth's magnetotail boundary, deviations of up to $\pm 20^\circ$ of ion bulk velocity from the antisolar direction have been seen [Intrilligator and Wolfe, 1973]. In spite of the fact that some decrease of ion bulk velocity is observed from variable ion spectra in the Martian magnetotail, the explanation of the observed decrease of currents requires either a considerable decrease of plasma density in the tail in comparison to the undisturbed solar wind (if such a decrease does occur, then it would be difficult to explain why electron currents in the magnetospheric tail are higher than those in the solar wind) or considerable deflection ($\sim 30^\circ$ – 40°) of the plasma bulk flow at the magnetopause. Therefore it seems that this boundary layer version is not very probable.

If a plasma sheet exists in the Martian magnetotail, then small fluxes registered may be explained by a high level of ion isotropy in this zone, similar in some way to conditions in earth's magnetotail. In this case there are no contradictions between simultaneous registration of low-ion and high-electron currents. In earth's magnetosphere, energies of isotropic plasma sheet ions are such that $\bar{E} > E_0$, where E_0 is the ion energy in the undisturbed solar wind and $\bar{E} \sim 6 \text{ keV}$ [Akasofu *et al.*, 1973]; but in the Martian magnetotail, $\bar{E} < E_0$. This difference might be caused by the fact that the Martian magnetic field is relatively weak and incapable of providing proper acceleration of ions.

The experimenters who performed measurements from Soviet Martian satellites by means of magnetometers and wide-angle plasma traps have always had the same opinion concerning the intrinsic magnetic field of Mars and its influence in

creating a near-planet bow shock [see *Gringauz et al.*, 1973b; *Dolginov et al.*, 1973; or see *Gringauz et al.*, 1975a; *Dolginov et al.*, 1975]. However, investigators using narrow-angle electrostatic analyzers [e.g., *Vaisberg et al.*, 1972] had differing opinions. *Vaisberg* [1974] concludes that even if the intrinsic magnetic field exists, it exerts little influence on the solar wind flowing around Mars.

Vaisberg and Bogdanov [1974] noted that inside the transition region on both the day and the night side of Mars a zone of hot plasma was detected which was essentially characterized by a decrease of the bulk velocity and was a continuation of the plasma flow behind the bow shock. The solar wind flow around Mars essentially differs from that around the earth by the existence of a viscous boundary layer deep within the transition region [*Vaisberg and Bogdanov*, 1974]. Further, these authors contend that the cause of the formation of this layer at the upper boundary of the ionosphere seems to be the viscous interaction with a dissipating outer envelope around Mars and that this kind of interaction of the solar wind with other bodies of the solar system had not previously been observed.

Vaisberg et al. [1975a, b] noted that the data from ion electrostatic analyzers aboard Mars 5 confirm conclusions made from Mars 2 and 3 data. They noted that when the spacecraft penetrated deep into the boundary layer, softening and decreasing of ion fluxes were simultaneously observed in all energy ranges down to below the instrument threshold sensitivity. As was mentioned, Mars 2 and 3 ion measurements were made only by means of electrostatic analyzers [e.g., *Vaisberg et al.*, 1972], while aboard Mars 5, ion measurements were also made with the Faraday cup. The data from Mars 5, as described by *Vaisberg et al.* [1975a, b], do not contradict results obtained by means of the Faraday cup. At the same time the interpretation of the data in the papers by *Vaisberg* [1974] and *Vaisberg and Bogdanov* [1974] raises serious objections. These authors tried to use the decrease and the gradual spectral softening of ion fluxes observed in the transition region (apparently, near the obstacle) as evidence for the non-magnetic nature of the obstacle and as a proof that ion fluxes in the transition layer interacted with particles dissipated from the Martian atmosphere.

However, quite similar phenomena also occur near the earth's magnetopause, and there is no doubt about the magnetic nature of the obstacle in the case of the earth. Results of experimental investigations of the earth's magnetopause have shown that there exists a boundary layer [*Hones et al.*, 1972], a 'plasma mantle' [*Rosenbauer et al.*, 1975], and a 'diffuse magnetopause' near the boundary of the magnetotail at all geomagnetic latitudes higher than those of the polar cusps [*Bezrukikh et al.*, 1975; *Hones et al.*, 1972; *Rosenbauer et al.*, 1975]. In the day side magnetosphere at low latitudes, ion fluxes are low in comparison to those in the transition layer, and their energy spectrum softens with decreasing radial distance in the same manner as occurs in near-Mars space [*Bezrukikh et al.*, 1975]. Therefore the explanation of effects described by *Vaisberg and Bogdanov* [1974] does not require the supposition of a nonmagnetic obstacle for Mars. There is no need to contend that such a new interaction of the solar wind with an obstacle has been found in the solar system for the first time.

Vaisberg and Bogdanov [1975] compare results obtained by means of narrow-angle electrostatic analyzers for the position of the bow shock to the results predicted by models based on a purely ionospheric obstacle without an intrinsic planetary magnetic field. Ionospheric bow shocks for Mars have been

discussed by *Spreiter et al.* [1970] and *Cloutier and Daniell* [1973], and for Venus by *Johnson and Midgley* [1969]. The applicability of these models to Mars was discussed above.

Recently, there have been changes in *Vaisberg's* views. *Rassbach et al.* [1974] developed a model based on the existence of an intrinsic Martian magnetic field. This model was included in the report by *Vaisberg et al.* [1975b] which was presented to the 1975 COSPAR symposium.

Vaisberg et al. [1975b] also report the detection of heavy ions ($Z > 2$) in the plasma flowing around Mars. This statement is based on a comparison of the results obtained from the Mars 5 satellite with some results of laboratory instrument tests which are not presented in the report. Therefore the conclusion about heavy ion detection is somewhat difficult to judge.

Vaisberg also criticizes considerations of the physical characteristics of plasma in the antisolar region of near-Mars space, as given by *Gringauz et al.* [1974c, 1975a, b] and presented above. *Vaisberg et al.* [1975b] suppose that in this region the ion fluxes are not proton fluxes but are instead heavy ion fluxes and that these heavy ions have a mean energy flux equal to that of the solar wind. Hence at constant ion density the ion flux is less than a pure proton flux by a factor of $m_i^{1/2}$. According to *Vaisberg's* estimates, this should reduce ion fluxes by a factor of 5. *Vaisberg's* report also stated that the wide-angle ion trap on the sunward side of the spacecraft for some reason collected fewer ions in the boundary layer (in the magnetotail) than in the solar wind and that the influence of photoelectrons on the electron trap readings in the boundary layer is different from that in the solar wind. Since *Vaisberg et al.* did not argue this point, we shall not consider it. However, the properties of traps were considered in detail in section 2 of this review.

5. CONCLUSIONS

Plasma measurements aboard the satellites Mars 2, 3, and 5 in the near-Mars space were conducted by means of charged particle traps. The measurements of the electron component of the plasma were made by the retarding potential method on all satellites, while measurements of the ion component were made only on Mars 5 by the modulation (Faraday cup) method. A bow shock and variations of its position relative to the planet, as well as interplanetary shock waves, were observed at the orbit of Mars. The satellite Mars 5 not only crossed the bow shock and the transition region but also entered the obstacle that creates the bow shock. Measurements performed on the antisolar side of Mars inside the obstacle revealed probably quasi-isotropic plasma. The measurements further lead to the conclusion that the subsolar point of the bow shock can move through distances of up to $\sim 1 R$ relative to the planet (depending on the solar wind ram pressure). Arguments are given favoring such a range of bow shock positions if Mars has an intrinsic dipole magnetic field. Plasma and geometric characteristics of Martian ionosphere according to Mariner 9 and other Martian satellites show that the ionosphere is stable and apparently not influenced by solar wind variations. The models published thus far of the solar wind flow around Mars based on a purely ionospheric obstacle cannot explain the creation of bow shocks as distant from the planet as they were observed to be in a number of cases from the satellites of Mars.

The totality of the magnetic field and plasma results leads to the conclusion that Mars possesses an intrinsic magnetic field

and that there probably exists a zone of quasi-isotropic plasma in the tail of the Martian magnetosphere.

Acknowledgments. I would like to thank A. A. Galeev of the Space Research Institute for useful discussions and James Carbary and A. J. Dessler of Rice University in Houston, Texas, for their help in the preparation of the final typescript.

REFERENCES

- Akasofu, S. I., E. W. Hones, Jr., S. J. Bame, J. R. Asbridge, and A. T. Y. Lui, Magnetotail and boundary layer plasmas at a geocentric distance of $\sim 18 R_E$: Vela 5 and 6 observations, *J. Geophys. Res.*, **78**(31), 7257, 1973.
- Bezrukikh, V. V., T. K. Breus, P. A. Maisuradze, A. P. Remizov, E. K. Solomatina, and M. I. Verigin, Dependence of the earth's magnetopause and bow shock positions on the solar wind parameters and the magnetopause plasma aboard the Prognoz and Prognoz 2 satellites, *Rep. D-192*, Space Res. Inst., Moscow, 1975.
- Bogdanov, A. V., O. L. Vaisberg, N. F. Borodin, A. A. Zertsalov, B. V. Polenov, and S. Romanov, Solar plasma interaction with Mars: Preliminary results, *Icarus*, **18**, 59, 1973.
- Breus, T. K., and M. I. Verigin, Study of solar plasma and along the earth to Mars path by means of charged particle traps aboard the Soviet spacecraft, 4, The comparison of the results of simultaneous plasma and magnetic measurements aboard the Mars 2 satellite, paper presented at Symposium of IAGA S-18, Grenoble, France, August 1975.
- Bridge, H. S., A. J. Lazarus, J. D. Scudder, K. W. Ogilvie, R. E. Hartle, J. R. Asbridge, S. J. Bame, W. C. Feldman, and G. L. Siscoe, Observations at Venus encounter by the plasma science experiment on Mariner 10, *Science*, **183**, 1293, 1974.
- Cloutier, P. A., and R. E. Daniell, Ionospheric currents induced by solar wind interaction with planetary atmospheres, *Planet. Space Sci.*, **21**, 463, 1973.
- Cloutier, P. A., M. B. McElroy, and F. C. Michel, Modification of the Martian ionosphere by solar wind, *J. Geophys. Res.*, **74**, 6215, 1969.
- Dolginov, Sh. Sh., E. G. Eroshenko, L. N. Zhuzgov, The magnetic field in the finite of the Mars according to the data from the Mars-2 and the Mars-3 (in Russian), *Dokl. Akad. Nauk SSSR*, **207**, 1296, 1968.
- Dolginov, Sh. Sh., L. N. Zhuzgov, and E. G. Eroshenko, Magnetic field in the very close neighborhood of Mars according to data from the Mars 2 and the Mars 3 spacecraft, *J. Geophys. Res.*, **78**, 4779, 1973.
- Dolginov, Sh. Sh., L. N. Zhuzgov, and E. G. Eroshenko, The magnetic field in the finite of the Mars according to the data from the Mars 3 and Mars 5 satellites (in Russian), *Kosm. Issled.*, **13**, 1, 1975.
- Fairfield, D. H., Average and unusual locations of the earth's magnetopause and bow shock, *J. Geophys. Res.*, **76**, 6700, 1971.
- Gringauz, K. I., Low-energy plasma in the earth's magnetosphere, *Rev. Geophys. Space Phys.*, **7**, 339, 1969.
- Gringauz, K. I., V. V. Bezrukikh, G. I. Volkov, T. K. Breus, L. S. Musatov, L. P. Havkin, and G. F. Sloutchenkov, Preliminary results on plasma electrons from Mars 2 and Mars 3, *Icarus*, **18**, 54, 1973a.
- Gringauz, K. I., V. V. Bezrukikh, T. K. Breus, G. I. Volkov, L. S. Musatov, L. P. Havkin, and G. F. Sloutchenkov, Results of solar plasma electron observations on Mars 2 and Mars 3 spacecraft, *J. Geophys. Res.*, **78**, 5808, 1973b.
- Gringauz, K. I., V. V. Bezrukikh, G. I. Volkov, M. I. Verigin, L. N. Davitaev, V. F. Kopylov, L. S. Musatov, and G. F. Sloutchenkov, Study of solar plasma near Mars and along earth to Mars path by means of charged particle traps aboard the Soviet spacecrafts, launched in 1971-1973, 1, Techniques and devices (in Russian), *Kosm. Issled.*, **12**(3), 430, 1974a.
- Gringauz, K. I., V. V. Bezrukikh, T. K. Breus, M. I. Verigin, G. I. Volkov, and A. V. Daychkov, Study of solar plasma near Mars and along the path earth-Mars by means of charged particle traps on Soviet spacecrafts, 1971-1973, 2, Characteristics of electron component along orbits of artificial satellites of Mars (Mars 2 and Mars 3) (in Russian), *Kosm. Issled.*, **12**(4), 585, 1974b.
- Gringauz, K. I., V. V. Bezrukikh, M. I. Verigin, and A. P. Remizov, Plasma at the antisolar part of near-Martian space as measured aboard the satellite Mars-5 (in Russian), *Dokl. Akad. Nauk SSSR*, **218**(4), 791, 1974c.
- Gringauz, K. I., V. V. Bezrukikh, M. I. Verigin, and A. P. Remizov, Study of solar plasma near Mars and along the earth to Mars path by means of charged particle traps aboard the Soviet spacecrafts launched in 1971-1973, 3, Characteristics of ion and electron plasma components in antisolar part of the near-Martian space as measured aboard the satellite Mars-5 (in Russian), *Kosm. Issled.*, **13**, 1, 1975a.
- Gringauz, K. I., V. V. Bezrukikh, M. I. Verigin, L. I. Denstchikova, V. I. Karpov, V. F. Kopylov, Yu. I. Krisilov, and A. P. Remizov, Measurements of electron and ion plasma components along the Mars-5 satellite orbit, *Rep. D-194*, Space Res. Inst., Acad. of Sci., USSR, Moscow, 1975b.
- Heath, D. E., Space observations of the variability of solar irradiance in the near and far ultraviolet, *J. Geophys. Res.*, **78**, 2779, 1973.
- Holzer, R. E., J. G. Northrop, J. V. Olson, and C. T. Russell, Study of waves in the earth's bow shock, *J. Geophys. Res.*, **77**, 2264, 1972.
- Hones, E. W., Jr., J. R. Asbridge, S. J. Bame, M. D. Montgomery, S. Singer, and S. I. Akasofu, Measurements of magnetotail plasma flow made with Vela 4B, *J. Geophys. Res.*, **77**(28), 5503, 1972.
- Hundhausen, A. J., *Coronal Expansion and Solar Wind*, Springer, New York, 1972.
- Intrilligator, D. S., and J. H. Wolfe, Evidence of a diffuse magnetopause boundary, *J. Geophys. Res.*, **77**(28), 5480, 1973.
- Johnson, F. S., and J. E. Midgley, Induced magnetosphere of Venus, *Space Res.*, **9**, 760, 1969.
- Kliore, A. J., D. L. Gain, G. Fjeldbo, B. L. Seidel, and S. I. Rasool, Mariner 9 S-Band Martian occultation experiment initial results on the atmosphere and topography of Mars, *Science*, **175**, 313, 1972.
- Kliore, A. J., G. Fjeldbo, B. L. Seidel, M. J. Sykes, and P. M. Woiceshyn, S Band radio occultation measurements of the atmosphere and topography of Mars with Mariner 9: Extended mission coverage of polar and intermediate latitudes, *J. Geophys. Res.*, **78**, 4331, 1973.
- Michel, F. C., Solar wind interaction with planetary atmospheres, *Rev. Geophys. Space Phys.*, **9**(2), 427, 1971.
- Montgomery, M. D., S. J. Bame, and A. J. Hundhausen, Solar wind electrons: Vela 4 measurements, *J. Geophys. Res.*, **73**, 4999, 1968.
- Ness, N. F., K. W. Behannon, R. P. Lepping, Y. C. Whang, and K. H. Schatten, Magnetic field observations near Venus: Preliminary results from Mariner 10, *Science*, **183**, 1301, 1974.
- Neugebauer, M., C. T. Russell, and J. V. Olson, Correlated observations of electrons and magnetic field of the earth's bow shock, *J. Geophys. Res.*, **76**, 4366, 1971.
- Obayashi, T., Interaction of solar plasma streams with the outer geomagnetic field, *J. Geophys. Res.*, **69**, 861, 1964.
- Olbert, S., Summary of experimental results from MIT detector on Imp-1, in *Physics of the Magnetosphere*, edited by R. L. Carovillano, D. Reidel, Dordrecht, Netherlands, 1968.
- Rassbach, M. E., R. A. Wolf, and R. E. Daniell, Convection in a Martian magnetosphere, *J. Geophys. Res.*, **79**, 1125, 1974.
- Rosenbauer, H., H. Grunwald, M. D. Montgomery, G. Paschmann, and N. Sckopke, Heos 2 plasma observations in the distant polar magnetosphere: The plasma mantle, *J. Geophys. Res.*, **80**(19), 2723, 1975.
- Spreiter, J. R., and A. W. Rizzi, The Martian bow wave—Theory and observation, *Planet. Space Sci.*, **20**, 205, 1972.
- Spreiter, J. R., A. L. Summers, and A. W. Rizzi, Solar Wind flow past nonmagnetic planets—Venus and Mars, *Planet. Space Sci.*, **18**, 1281, 1970.
- Vaisberg, O. L., A new information on plasma envelopes of Mars and Venus (in Russian), *Zemlya Vseleennaya*, **2**, 19, 1974.
- Vaisberg, O. L., and A. V. Bogdanov, The flow past Mars and Venus by solar wind: General regularity (in Russian), *Kosm. Issled.*, **12**, 279, 1974.
- Vaisberg, O. L., and A. V. Bogdanov, Structure and variations of solar wind-Mars interaction region, *J. Geophys. Res.*, **80**(4), 487, 1975.
- Vaisberg, O. L., A. V. Bogdanov, N. F. Borodin, A. A. Zertsalov, B. V. Polenov, and S. A. Romanov, Observations of the region of interaction of solar wind plasma to the Mars (in Russian), *Kosm. Issled.*, **9**, 462, 1972.
- Vaisberg, O. L., A. V. Bogdanov, N. F. Borodin, A. V. Djachkov, A. A. Zetsalov, I. P. Karpinsky, K. P. Kondakov, Z. N. Mamotko, B. V. Polenov, S. A. Romanov, and V. N. Smirnov, The measurements of low-energy particles aboard the interplanetary stations Mars-2 and Mars-3 (in Russian), *Kosm. Issled.*, **11**, 743, 1973.
- Vaisberg, O. L., A. V. Bogdanov, V. N. Smirnov, and S. A. Romanov, First results of measurements of ion fluxes by device RIEP-280IM aboard the Mars-4 and Mars-5 (in Russian), *Kosm. Issled.*, **13**, 129, 1975a.
- Vaisberg, O. L., V. N. Smirnov, A. V. Bogdanov, A. P. Kalinin, J. P.

- Karpinsky, B. V. Polenov, and S. A. Romanov, Ion flux parameters in the region of solar wind interaction with Mars according to measurements of Mars 4 and Mars 5, *Rep. D-191*, Space Res. Inst., Acad. of Sci., USSR, Moscow, 1975b.
- Whipple, E. C., and L. V. Parker, Effects of secondary electron emission on electron trap measurements in the magnetosphere and solar wind, *J. Geophys. Res.*, **74**, 5763, 1969.

(Received September 10, 1975;
accepted January 9, 1976.)